Published in final edited form as:
Cell Calcium. 2008 December ; 44(6): 604–615. doi:10.1016/j.ceca.2008.05.001.

Synergistic Regulation Of Endogenous TRPM2 Channels By Adenine Dinucleotides In Primary Human Neutrophils

Ingo Lange, **Reinhold Penner**, **Andrea Fleig***, and **Andreas Beck**
Laboratory of Cell and Molecular Signaling, Center for Biomedical Research at The Queen's Medical Center and John A. Burns School of Medicine at the University of Hawaii, Honolulu, Hawaii 96813

Summary

The Ca^{2+}-permeable TRPM2 channel is a dual function protein that is activated by intracellular ADPR through its enzymatic pyrophosphatase domain with Ca^{2+} acting as a co-factor. Other TRPM2 regulators include cADPR, NAADP and H_2O_2, which synergize with ADPR to potentiate TRPM2 activation. Although TRPM2 has been thoroughly characterized in overexpression or cell-line systems, little is known about the features of TRPM2 in primary cells. We here characterize the regulation of TRPM2 activation in human neutrophils and report that ADPR activates TRPM2 with an effective half-maximal concentration (EC_{50}) of 1 μM. Potentiation by Ca^{2+} is dose-dependent with an EC_{50} of 300 nM. Both cADPR and NAADP activate TRPM2, albeit with lower efficacy than in the presence of subthreshold levels of ADPR (100 nM), which significantly shifts the EC_{50} for cADPR from 44 μM to 3 μM and for NAADP from 95 μM to 1 μM. TRPM2 activation by ADPR can be suppressed by AMP with an IC_{50} of 10 μM and cADPR-induced activation can be blocked by 8-Bromo-cADPR. We further show that 100 μM H_2O_2 enables subthreshold concentrations of ADPR (100 nM) to activate TRPM2. We conclude that agonistic and antagonistic characteristics of TRPM2 as seen in overexpression systems are largely compatible with the functional properties of TRPM2 currents measured in human neutrophils, but the potencies of agonists in primary cells are significantly higher.

Introduction

The widely expressed Na^+- and Ca^{2+}-permeable cation channel TRPM2 functions both as an ion channel and an ADP-ribose (ADPR)-specific pyrophosphatase [1-6]. The primary channel-gating mechanism is mediated by ADPR [4,7], although limited activation of TRPM2 can be accomplished by H_2O_2 [2,8,9] and relatively high concentrations of cyclic ADP-ribose (cADPR) [7,10,11]. However, cADPR, and H_2O_2 can synergize with ADPR to activate TRPM2 currents at ADPR levels in the low nanomolar range [7], although one report has claimed that this does not seem to be the case for human neutrophils [12]. Another activator of TRPM2 channels in overexpressing HEK293 cells and Jurkat T lymphocytes is the highly efficient Ca^{2+}-release agent nicotinic acid adenine dinucleotide phosphate (NAADP, [13]), which can also facilitate ADPR action on TRPM2 [10]. At the same time, the channel's sensitivity to ADPR is potentiated by intracellular Ca^{2+} [4,12,14-16] acting as a positive feedback mechanism on channel activity, likely mediated by calmodulin [16,17]. Furthermore,

*Correspondence should be addressed to: Andrea Fleig, PhD, 1301 Punchbowl Street, Honolulu, Hi 96813. Fax: 808-537-7939; E-mail: afleig@hawaii.edu.

TRPM2 most likely has a direct Ca^{2+}-binding site that is accessible from either side of the membrane and must be occupied by Ca^{2+} for proper channel function [16]. Ca^{2+}-dependence of TRPM2 activity has been reported in a variety of cell lines [4,12,14-16,18], as well as in primary systems such as neutrophil granulocytes [12].

At present, little is known about the interaction between ADPR, cADPR, NAADP and intracellular Ca^{2+} in a primary cell system [19]. Endogenous TRPM2 currents measured in a primary cell system were first described in human neutrophil granulocytes [20]. Perfusing these cells with 300 μM ADPR and intracellular Ca^{2+} clamped close to 0 using EGTA evoked single channel currents that could be resolved at the whole-cell level and showed characteristics of TRPM2 with long open times and a large conductance of 56 pS [20]. In microglia cells isolated from brain [21], application of 5 mM H_2O_2 or perfusing cells with a single fixed ADPR concentration of 1 mM evoked whole-cell currents and single channel activity typical for TRPM2 [4]. Other primary cell systems that have been assessed for TRPM2 currents are mouse megakaryocytes [22] and rat striatal neurons [23]. In megakaryocytes, 1 mM ADPR in the presence of 1 μM intracellular Ca^{2+} evoked TRPM2 currents that were not seen in the absence of Ca^{2+} [22]. On the other hand, 500 μM ADPR activated TRPM2 currents in rat striatal neurons even when buffering intracellular Ca^{2+} close to 0 using 500 μM EGTA [23]. Further studies on hippocampal CA1 neurons using Ca^{2+} imaging in an *in vivo* oxygen-glucose deprivation model [24], and studies on primary rat pancreatic beta cells measuring heat-activated calcium signals [11] imply a role of TRPM2 in these systems but do not provide patch-clamp recordings for these two primary cell types.

To gain a more detailed understanding of TRPM2 characteristics in a primary cell system, we initially probed three immune cell types for ADPR-induced TRPM2 currents, namely mouse bone marrow-derived mast cells, naïve human T lymphocytes and human neutrophils. Since only human neutrophils developed ADPR-induced currents, we concentrated on this primary cell model to investigate the efficacy of known TRPM2 agonists and modulators as well as TRPM2 antagonists AMP and 8-Bromo-cADPR using K^+-based intracellular conditions.

Methods

Cell Culture

Isolation of human neutrophils and T cells—Human neutrophils and T cells were obtained from whole human blood donated by volunteers with protocol approval from The Queen's Medical Center Research & Institutional Committee. Human neutrophils were isolated using a Dextran-500 sedimentation (Amersham Bioscience 17-0320-01), followed by a Ficoll Paque Plus density centrifugation (Amersham GE, Piscataway, NJ). Cells were positively selected using Macs CD15 Microbeads (130-046-601, Miltenyi Biotec GmbH, Germany). Isolated cells were kept in a medium containing RPMI and 10% fetal bovine serum at 37 °C in an incubator. Experiments were started 1 hour after isolation. To this end, 500 μl of cells were transferred into an Eppendorf tube, diluted with 500 μl external Na^+-Ringer, centrifuged and resuspended in 500 μl Na^+-Ringer. Human T cells were isolated using the RosetteSep™ protocol according to manufacturer's instructions (StemCell Technologies Inc., Vancouver, Canada). Cells isolated this way were kept in standard RPMI tissue culture medium supplemented with 10% FBS at 37 °C until used for patch-clamp experiments.

Isolation of mouse bone marrow-derived mast cells (BMMC)—Mouse BMMCs were isolated from adult mice 20 g and heavier as described previously [25] and with protocol approval from the University of Hawaii Institutional Animal Care and Use Committee.

Solutions

For patch-clamp experiments, cells were kept in standard external solution (in mM): 140 NaCl, 2.8 KCl, 1 $CaCl_2$, 2 $MgCl_2$, 11 glucose, 10 HEPES·NaOH (pH 7.2 adjusted with NaOH, 300-320 mOsm). Standard pipette-filling solutions contained (in mM): 140 K-glutamate, 8 NaCl, 1 $MgCl_2$, 10 HEPES·KOH (pH 7.2 adjusted with KOH, 290-310 mOsm). ADPR, cADPR, NAADP, H_2O_2 or a combination thereof was added to the standard internal solution. $[Ca^{2+}]_i$ was buffered to 0, 100, 200, 300, 500 or 1000 nM with 10 mM BAPTA and 0, 3.1, 4.7, 5.7, 6.9 or 8.2 mM $CaCl_2$, respectively, calculated with WebMaxC (http://www.stanford.edu/~cpatton/webmaxcS.htm) or left unbuffered (no Ca^{2+} buffer present). All chemicals except BAPTA (Invitrogen-Molecular Probes, Carlsbad, CA) were purchased from Sigma-Aldrich, USA.

Electrophysiology—Patch-clamp experiments were performed in the whole-cell configuration at 25 °C. Patch pipettes were pulled from Kimax glass capillaries (Kimble Products, Fisher Scientific, USA) on a DMZ-Universal Puller (DAGAN, Minneapolis, MN), and had resistances of 1.5-3 MΩ. Data were acquired with Pulse and PatchMaster software controlling an EPC-9 amplifier. Voltage ramps of 50 ms spanning the voltage range of −100 to +100 mV were delivered at a rate of 0.5 Hz, typically over a period of 100 s. The holding potential was 0 mV to suppress depolarization-induced SK channels. Voltages were corrected for a liquid junction potential of 10 mV. Currents were filtered at 2.9 kHz and digitized at 100 μs intervals. The low-resolution temporal development of currents for a given potential was extracted from individual ramp current records by measuring the current amplitudes at voltages of −80 mV. Data were analyzed using PulseFit or FitMaster (HEKA, Lambrecht, Germany), and IgorPro (WaveMetrics, Lake Oswego, Or). Data were exported from PulseFit or FitMaster without leak subtraction. Currents were normalized to cell size in pF. Basal currents were taken from the averaged and normalized current plateau phase at a compound concentration that did not activate TRPM2 currents (100 nM ADPR, 300 nM cADPR, 0 Ca^{2+}). Background currents ranged between −5 and −15 pA/pF at −80 mV. The average cell size of human neutrophils was 2.3 ± 0.08 pF (n = 40), of BMMC's 6.8 ± 1 pF (n = 4) and human T lymphocytes 1.7 ± 0.05 pF (n = 75). Where applicable, statistical errors of averaged data are given as means ± S.E.M. with n determinations. Single ramps were plotted as current-voltage relationships (IVs) and were not leak-subtracted.

Fura-2 Ca^{2+} measurements and perforated patch—For Ca^{2+} measurements, cells were loaded with 5 μM Fura-2-AM (acetoxymethylester, Molecular Probes) for 30 min in media at 37 °C. Using Fura-2-AM pre-loaded cells, perforated-patch clamp experiments were performed where the internal solution was supplemented with 200 μm Fura-2 and 300 μM amphotericin B (Sigma, freshly prepared from 30 mM stock in DMSO). To this end, cells were kept in the cell-attached mode at a holding potential of 0 mV until the series resistance was less than 20 MΩ (within 10 min), then the standard ramp protocol (see above) was started.

The cytosolic calcium concentration of individual patch-clamped cells was monitored at a rate of 5 Hz with a dual excitation fluorometric system using a Zeiss Axiovert 200 fluorescence microscope equipped with a 40x LD AchroPlan objective. The monochromatic light source (monochromator B, TILL-Photonics) was tuned to excite Fura-2 fluorescence at 360 and 390 nm for 20 ms each. Emission was detected at 450-550 nm with a photomultiplier, whose analog signals were sampled and processed by X-Chart software (HEKA, Lambrecht, Germany). Fluorescence ratios (F_{360}/F_{390}) were translated into free intracellular calcium concentration based on calibration parameters derived from patch-clamp experiments with calibrated Ca^{2+} concentrations.

Single-channel measurements—Single-channel recordings were performed in the whole-cell configuration using standard external solutions. For single-channel acquisition, K^+ ions were replaced with cesium (Cs^+). A threshold concentration of 100 nM or 200 nM ADPR in unbuffered intracellular conditions was used to evoke a low level of channel activity. Ramps from −100 mV to 100 mV over 20 s were applied continuously, recorded at a gain of 50 mV/pA and filtered at 50 Hz. Due to the slight outward rectification visible in the measurements, linear fits to the data were performed from either −100 mV to 0 mV or from 0 mV to +100 mV to evaluate the single channel conductance in pS.

Results

Regulation of TRPM2 by intracellular Ca^{2+}

We have previously reported that cADPR, H_2O_2, and NAADP can synergize with the primary agonist ADPR to more efficiently activate TRPM2 [7] and we recently demonstrated in Jurkat T cells and HEK293 cells overexpressing TRPM2 that intracellular cations can affect the sensitivity of TRPM2 channels to ADPR and cADPR [7,10], which might also affect the synergistic effects of other TRPM2 modulators. Previous studies on TRPM2 in primary neutrophils employed Cs^+-based intracellular solutions [12,20], and one study reported the failure of cADPR to activate or synergize with ADPR and AMP to inhibit ADPR-induced TRPM2 currents in human neutrophils [12]. Since these studies provided results under somewhat limited experimental conditions, we conducted a detailed analysis of the facilitatory actions of cADPR, H_2O_2 and NAADP in relation to ADPR-induced TRPM2 activation in primary human neutrophils, using K^+-based solutions and assessing agonist effects over a large concentration range.

We first set out to construct an ADPR dose-response curve in neutrophils isolated from whole human blood. Figure 1A shows the average normalized time course of inward currents measured in neutrophils at −80 mV and evoked by increasing concentrations of intracellular ADPR (100 nM – 1 mM) added to the standard K^+-glutamate based pipette solution. The intracellular calcium concentration ($[Ca^{2+}]_i$) was left unbuffered by omission of any exogenous Ca^{2+} chelators, since clamping $[Ca^{2+}]_i$ to about zero with 10 mM BAPTA prevented activation of TRPM2 even in the presence of 1 mM ADPR (data not shown). This caused a dose-dependent activation of ADPR-dependent currents that showed typical properties of TRPM2 with a linear current-voltage (I/V) relationship and a reversal potential (E_{rev}) at 0 mV (Fig. 1C). To establish the dose-response curve of ADPR-induced currents, the maximum ADPR-evoked currents measured at 100 s into the experiment were extracted, averaged, normalized to cell size and plotted versus their respective ADPR concentration (Fig. 1D; black circles, n = 4-10). A dose-response fit to the data yielded a half-maximal effective concentration (EC_{50}) for ADPR of 1.1 μM with a Hill coefficient of 1.5. This is considerably lower than the EC_{50} values obtained for heterologously expressed TRPM2 in HEK293 cells (10 μM) [7, 16], or native TRPM2 in Jurkat T cells (7 μM) [10], U937 monocytes (40 μM) [4], and RINm5f cells (20 μM, Fleig unpublished observations), indicating that both ionic and cellular environment can determine the sensitivity of TRPM2 channels to ADPR.

Several cellular systems have been shown to require the presence of intracellular and/or extracellular Ca^{2+} to evoke ADPR-induced TRPM2 currents, including human neutrophils [4,12,14-16]. When perfusing human neutrophils with a fixed concentrations of 1 mM ADPR in the presence of increasing intracellular Ca^{2+} concentrations ranging from 0 to 1 μM (Fig. 1B; n = 5-9), TRPM2 currents reached peak current amplitude faster than in unbuffered conditions (see Fig. 1A), within 10-20 s. Typically, these currents also inactivated by about 20% within the time frame of the experiments. Fitting a dose-response curve to the average normalized currents measured at the peak showed that the Ca^{2+} concentration required for half-

maximal activation of TRPM2 at 1 mM ADPR was 300 nM with a Hill coefficient of 2 (Fig. 1D; red circles, n = 5-9).

ADPR-induced activation of TRPM2 currents are negatively regulated by increasing intracellular AMP concentrations in Jurkat T cells and HEK293 cells overexpressing the channel [7,10]. However, lower concentrations of AMP (5 μM) reportedly failed to inhibit TRPM2 in neutrophils activated by saturating ADPR concentrations (5 μM) in intracellular Cs^+ conditions [12]. We therefore evaluated the inhibitory action of AMP at 1 μM ADPR, the EC_{50} for this second messenger in neutrophils. As can be seen in Fig. 1E, 100 μM AMP substantially suppressed the activation of TRPM2 currents, indicating that AMP has the potential to inhibit ADPR-mediated TRPM2 activity when produced in excess of ADPR. We constructed a full concentration-response curve with various AMP concentrations in the presence of 1 μM ADPR. This revealed an IC_{50} for AMP of 10 μM with a Hill coefficient of 2 (Fig. 1F). In summary, the results presented in Figure 1 show that ADPR activates TRPM2 currents very effectively in a dose-dependent manner in primary human neutrophils. Furthermore, this activation is dependent on and facilitated by intracellular Ca^{2+} and counteracted by AMP.

Results from HPLC analysis indicate that the basal ADPR concentration of human neutrophils is around 5 μM and this value is not significantly altered by fMLP-induced receptor stimulation [12]. ADPR-induced TRPM2 activation requires intracellular calcium levels higher than 100 nM (Fig. 1B) and the EC_{50} for TRPM2 activation is around 1 μM in the presence of Ca^{2+} (Fig. 1D and [12]). We therefore reasoned that increasing the intracellular calcium concentration alone should activate TRPM2 current in a perforated-patch situation, where cellular ADPR levels would be left unperturbed. To this end we performed combined perforated-patch and Fura-2 experiments, where cells were first preloaded with Fura-2-AM and subsequently patched with the standard intracellular solution containing 300 μM amphotericin B (see methods). The pipette potential was kept at 0 mV. Upon establishment of the perforated-patch ($Rs < 20\ M\Omega$), the standard voltage ramp was started (see methods) and ionomycin (2 μM) was applied 20 s thereafter for a total of 5 s (Fig. 2A). While this induced a rapid increase of intracellular calcium of around 300 nM (Fig. 2A lower trace), it did not cause a concomitant activation of TRPM2 currents as observed over a time span of 200 s (Fig. 2A, upper trace). This indicates that either the local calcium concentration in the vicinity of TRPM2 channels does not reflect the global calcium increase or, alternatively, the local ADPR concentration is lower than 5 μM.

ADPR-activated single channel conductance of TRPM2 reportedly is between 56 pS and 67 pS, exhibiting characteristically long open times of up to tenths of seconds [4,10,14,20]. In neutrophils, application of 300 μM ADPR evoked a 56 pS single channel conductance typical for TRPM2 in excised inside-out patches at negative potentials [20]. To evaluate TRPM2 single-channel conductance, we performed whole-cell experiments perfusing neutrophils with threshold concentrations of ADPR to evoke low-level activity of individual channels and using a ramp protocol spanning −100 mV to +100 mV over 20 s. While 100 nM ADPR perfusion caused activity of two channels in 2 out of 6 cells (data not shown), increasing ADPR to 200 nM reliably activated two to five channels in 6 out of 6 cells. Figure 2B shows four consecutive ramp measurements of TRPM2 single channel activity recorded in a representative cell directly after whole-cell establishment (Fig. 2B, first trace at 0 s) and at 22 s, 44 s and 66 s into the experiment. All data traces were leak-corrected by subtracting the first null-trace (no channel activity) obtained directly after whole-cell break-in. Activity of two channels can be seen, with second-long open times, a reversal potential of 0 mV and a slight outward rectification. The current could not be adequately fitted with a linear regression across the whole voltage range, since outward currents exhibited steeper rectification. Therefore, two linear regression fits were

performed for positive potentials (0 to 100 mV) and negative potentials (0 to −100 mV) with a single-channel conductance of 63 ± 2 pS (n = 3) and 43 ± 0.4 pS (n = 3), respectively.

TRPM2-like currents or H_2O_2-induced Ca^{2+} influx linked to TRPM2 channels have been shown in various cell lines and primary tissues, including isolated mouse microglia, primary rat cerebral cortical neurons, monocytes, beta pancreatic cell lines and Jurkat T lymphocytes [19]. Since Jurkat T lymphocytes are a well-known model to study T-cell physiology, we wondered whether primary T lymphocytes isolated from whole human blood would also show ADPR-induced TRPM2 currents. However, when perfusing human naïve T lymphocytes from peripheral blood with 1 mM ADPR in standard K^+-glutamate based and Ca^{2+}-unbuffered solution, we never observed any TRPM2-like currents (Supplemental Data Fig. S1; open circles, n = 10). This also held true for another immune cell system, mouse mast cells derived from bone marrow (Supplemental Data Fig. S1; closed circles, n = 4). This indicates that TRPM2 channels are absent in the plasma membrane of these two cell types. However, the results do not preclude TRPM2 expression in other subcellular structures or in specific T cell subtypes.

Regulation of TRPM2 by cADPR and H_2O_2

TRPM2 currents measured in overexpressing HEK293 cells and Jurkat T lymphocytes can be activated by perfusion of cells with increasing cADPR concentrations, albeit at a significantly lower efficiency and reduced amplitude compared to ADPR, unless those two agents are co-perfused and synergize [7,10]. Since a previous report questioned the ability of cADPR to activate or synergize with native TRPM2 in human neutrophils [12], we addressed this issue by performing a detailed dose-response analysis of TRPM2 currents evoked by increasing cADPR concentrations between 300 nM and 1 mM added to our standard K^+-glutamate internal solution (Fig. 3A). We then plotted the average normalized maximum current measured at 100 s against the respective cADPR concentration and fitted the data with a dose-response curve. This established that cADPR activates TRPM2 currents with an EC_{50} of 44 μM and a Hill coefficient of 1 (Fig. 3D, blue circles, n = 4-9). This EC_{50} was shifted about 15-fold to the left by merely adding a subthreshold concentration of 100 nM ADPR to the respective cADPR concentrations. This is shown in Fig. 3B, which plots the average normalized time course of TRPM2 activation evoked by perfusing cells with the standard K^+-glutamate solution supplemented with 100 nM ADPR and increasing cADPR concentrations varying between 100 nM and 100 μM. Whereas 1 mM of cADPR was needed to fully activate TRPM2 currents, only 100 μM cADPR was required in the presence of subthreshold 100 nM ADPR (Fig. 3A and Fig. 3B). Fig. 3C illustrates I/V curves extracted at 100 s from representative neutrophils perfused with either 1 mM cADPR (black trace), 3 μM cADPR (blue trace) or a combination of 100 nM ADPR plus 3 μM cADPR (red trace). Plotting the average normalized current evoked by 100 nM ADPR plus increasing cADPR against the respective cADPR concentration resulted in a dose-response curve whose fit yielded an EC_{50} of 3 μM with a Hill coefficient of 2 (Fig. 3D, red circles, n = 5-7). This demonstrates that cADPR is able to enhance the effectiveness of subthreshold ADPR levels to efficacy levels that are almost comparable to ADPR-induced TRPM2 activation (EC_{50} = 1.1 μM, see Fig. 1C and 3D; Table 1).

It has previously been shown that H_2O_2 activates TRPM2 currents, although in a limited fashion [2,8,9]. Our work suggests that the effects of H_2O_2 on TRPM2 may be very similar to those of cADPR, in that both compounds are able to potentiate ADPR-induced TRPM2 activation [7]. We therefore revisited the question whether H_2O_2 could facilitate ADPR-induced TRPM2 currents in human neutrophils. To this end, we first perfused cells with the standard K^+-glutamate-based solution supplemented with either 100 μM H_2O_2 (Fig. 3E, open squares, n = 6) or 100 nM ADPR (Fig. 3E, open circles (behind open squares), n = 6). Neither of these manipulations activated any significant TRPM2 currents within the observed time frame of the

experiment. However, co-perfusing the cells with 100 μM H_2O_2 and 100 nM ADPR was effective in activating TRPM2 (Fig. 3E, closed circles, n = 6). We next assessed whether cADPR-induced TRPM2 currents could be blocked by the competitive inhibitor 8-Bromo-cADPR, as we had reported previously for heterologously expressed TRPM2 in HEK293 cells and Jurkat T lymphocytes [7,10]. Indeed, co-perfusion of 30 μM cADPR and 100 μM 8-Bromo-cADPR completely suppressed activation of TRPM2 currents (Fig. 3F, red circles, n = 6). These data confirm that both the synergy of cADPR and H_2O_2 with ADPR and the antagonistic effect of 8-Bromo-cADPR on cADPR are present in primary human neutrophils, even at lower concentrations and thus with higher potency and efficacy.

Regulation of TRPM2 by NAADP

NAADP has gained significant interest as the most potent Ca^{2+}-release agonist described to-date, acting at low nanomolar concentrations [26]. We previously reported that NAADP can potentially activate TRPM2 in Jurkat T cells and the HEK293 cells overexpressing the channel, albeit in the high μM concentration range [10]. We demonstrated for the TRPM2-overexpression system that NAADP synergizes with ADPR in the low micromolar range [10]. Since TRPM2 activation in neutrophils is significantly more sensitive to both ADPR and cADPR stimulation, we wondered whether this would hold true for the activation of the current by intracellular NAADP. We therefore perfused human neutrophils with the standard K^+-glutamate based internal solution supplemented with increasing NAADP concentrations ranging between 3 μM – 1 mM. This resulted in a dose-dependent activation of currents (Fig. 4A) that showed the typical I/V behavior of TRPM2 (Fig. 4C, black trace). A fit to the maximum normalized currents extracted at 100 s into the experiment resulted in an EC_{50} of 95 μM and a Hill of 1.6 (Fig. 4D, black circles, n = 3-5), slightly less efficient than cADPR. Interestingly, when co-perfusing cells with a subthreshold ADPR concentration of 100 nM and increasing NAADP (Fig. 4B), TRPM2 activation was only facilitated at or below 30 μM NAADP, whereas NAADP levels above 30 μM failed to do so and the dose-response behavior was identical to NAADP alone. This is shown in Fig. 4D, where the red squares indicate the dose-response curve resulting from ADPR supplementation of NAADP at various concentrations (n = 5-9). The first EC_{50} ($EC_{50}1$) of the dose-response fit to the ADPR plus NAADP data extracted at 100 s whole-cell time was calculated to be 1.1 μM with a Hill coefficient of 3, whereas the second component, $EC_{50}2$, was 116 μM with a Hill coefficient of 2. Fig. 4C depicts example I/V curves taken at 100 s from a cell perfused with 3 μM NAADP only, which failed to activate any currents (blue trace), and a cell co-perfused with 3 μM NAADP in the presence of 100 nM ADPR (red trace). These data confirm that TRPM2 can be activated by NAADP in a primary cells system expressing TRPM2 channels in the plasma membrane. In addition, with an EC_{50} of 95 μM, NAADP is about 8-fold more effective in activating TRPM2 currents in neutrophils than it is in the overexpression system (EC_{50} of 730 μM) and possibly Jurkat T cells [10] (see Table 1).

Discussion

The current study presents a comprehensive investigation of synergistic and antagonistic interactions of molecules known to influence TRPM2 activation in primary human neutrophils. We here show that intracellular Ca^{2+} is required for ADPR-induced TRPM2 activation in primary human neutrophils with half-maximal potentiation observed at 300 nM $[Ca^{2+}]_i$. Furthermore, endogenous TRPM2 currents are very efficiently activated by ADPR in the low micromolar range in unbuffered Ca^{2+} conditions, representing a left-ward shift in sensitivity of about one order of magnitude compared to heterologously expressed channels. Similarly, TRPM2 can also be activated by cADPR and NAADP with 40-100 fold lower efficiency. In agreement with our previous work [10], but in contrast to a study by Luckhoff and colleagues [12], intracellular cADPR, H_2O_2 and NAADP synergize with subthreshold ADPR

concentrations (100 nM) to boost TRPM2 activation. Finally, we establish that in human neutrophils, AMP and 8-Bromo-cADPR, suppress ADPR and cADPR-induced TRPM2 currents, respectively.

The current study is the first detailed investigation of TRPM2 activity in response to ADPR and known co-activators of ADPR and inhibitors thereof in a primary cell system using K^+-based internal solutions. Ca^{2+} is well known to be an important co-activator of ADPR-induced TRPM2 currents [4,12,14-16]. From the available data in overexpression systems, the EC_{50} values for $[Ca^{2+}]_i$ range between 340 nM in Cs^+-based solutions [15] to about 40 nM in K^+-based solutions [16]. A dose-response curve for intracellular Ca^{2+} has not been conducted in other cell lines or primary cell systems, although Heiner et al. [12] reported a two-point measurement of either low (10 mM EGTA) or high (1 μM) intracellular Ca^{2+} on ADPR-induced TRPM2 responses in human neutrophils using Cs^+ as main intracellular ion. They showed that the EC_{50} for ADPR was about 1 μM in the presence of 1 μM $[Ca^{2+}]_i$, which is similar to our data using unbuffered Ca^{2+} conditions and K^+-based internal solutions. Although we surmise that $[Ca^{2+}]_i$ under unbuffered conditions is likely to remain below 1 μM, it seems that Cs^+ does not significantly affect the ADPR-sensitivity of TRPM2 in neutrophils, unlike in HEK293 and Jurkat T cells [10]. Our data further show that internal Ca^{2+} co-activates TRPM2 currents with an EC_{50} of 300 nM at maximal ADPR concentrations (Fig. 1D, red circles). Therefore, the present Ca^{2+} dose-response data, as well as data acquired in unbuffered conditions [16] and the results reported by Heiner et al. [12] together argue in favor of a picture where concentrations higher than 1 μM Ca^{2+} do not significantly potentiate ADPR effects. Thus, even high $[Ca^{2+}]_i$ by itself is not expected to activate TRPM2 currents at ADPR levels below 300 nM (Fig. 1D). Interestingly, although the overall ADPR concentrations in human neutrophils has been reported to be around 5 μM [12], the ADPR concentration in the vicinity of the channel seems to be below 300 nM, since raising intracellular calcium without disturbing intracellular basal ADPR levels does not cause TRPM2 activation (Fig. 2A).

Intracellular cADPR has been reported as a Ca^{2+}-release agent in various cell types [26] and recent data suggest a role in Ca^{2+} influx [27], which at least in part has been linked to TRPM2 activation [7,10,11]. In HEK293 cells overexpressing human TRPM2 channels, cADPR is quite inefficient in activating the channel with an EC_{50} of 700 μM in unbuffered Ca^{2+} and K^+-based conditions [10]. Jurkat T lymphocytes and human neutrophils, on the other hand, are at least 10-fold more sensitive to cADPR at otherwise identical experimental conditions ([10] and Fig. 3D). Only when exposing HEK293 cells overexpressing rat TRPM2 channels to 40 °C does cADPR reach an EC_{50} value of around 60 μM [11]. Importantly though, the presence of both ADPR and cADPR increases the effectiveness of TRPM2 activation in both heterologous and endogenous expression systems. While this observation has not been quantified in great detail for Jurkat T cells, the synergistic effect of ADPR and cADPR cooperativity at subthreshold levels impresses with a 100-fold shift in EC_{50} for TRPM2 activation in HEK293 cells (from 12 μM to 90 nM for ADPR; [7]) and a 15-fold shift in human neutrophils (from 44 μM to 3 μM for cADPR; Fig. 3D, red circles).

The ability of cADPR to activate TRPM2 currents may not directly be due to cADPR itself, but possibly to synergism with ADPR made available from other sources, such as contamination of the cADPR salt or ambient levels or metabolically produced ADPR from cADPR by cytosolic ADP-ribosyl cyclases [28]. Luckhoff and colleagues reported that in human neutrophils cADPR failed to activate TRPM2 currents even at 10 μM concentrations if the cADPR was pre-treated with pyrophosphatase to break down any ADPR contamination into ribose-5-phosphate and AMP [12]. ADPR contamination of the cADPR used in their study was estimated to be at 25%. The cADPR lot used in the present study had significantly lower contamination levels. HPLC data obtained from the manufacturer (Sigma-Aldrich, USA) determined that our lot of cADPR had 94.5% purity, with 4.2% contamination of NAD^+ or

nicotinamide and 1% contamination with other unidentified nucleotides, possibly including ADPR. This quantitative analysis is compatible with our functional assays. Assuming a 1% contamination of ADPR in our lot of cADPR, a 100-fold concentration of cADPR should have similar efficacy of activating TRPM2 currents if this were solely due to ADPR contamination in the absence of any facilitatory action of cADPR. However, this is not the case, as the EC_{50} for cADPR is around 40 μM rather than the expected 110 μM, indicating that cADPR synergizes with ADPR to enhance TRPM2 activity. This is further corroborated by adding subthreshold ADPR (100 nM) to increasing cADPR concentrations, which is sufficient to shift the EC_{50} value about 15-fold from 44 μM to 3 μM, close to the apparent EC_{50} for ADPR itself (1.1 μM, Fig. 3D).

The relatively high contamination levels of cADPR with 25% ADPR may also account for a further discrepancy between our work [7,10] and previous results [12]. The latter study did not observe any synergy of subthreshold ADPR (100 nM) and 10 μM cADPR, when cADPR was pre-treated with pyrophosphatases to remove the contaminating ADPR. This might be explained by the fact that such treatment will replace the contaminating ADPR with equal levels of its breakdown products. We have previously shown that, while ribose-5-phosphate does not interfere with TRPM2 activation by ADPR [7], AMP can inhibit ADPR-mediated activation of TRPM2 [7,10]. Furthermore, the data presented here show that a 100-fold surplus of AMP is quite effective in suppressing TRPM2 currents in the presence of 1 μM ADPR (Fig. 1E). Thus, when degrading ADPR using the pyrophosphatase, AMP levels would increase in the cADPR sample to similar levels of the previous ADPR contamination. With an estimated contamination level of 25% by ADPR [12], cADPR very likely would have contamination levels of 25% AMP after pyrophosphatase treatment. Hence, using 10 μM of pre-treated cADPR would contain around 2.5 μM AMP, which might be sufficient to suppress any effect caused by the additionally added 100 nM ADPR. The presence of AMP in the pre-treated cADPR sample may also explain the absence of cADPR effects on TRPM2 observed previously in neutrophils [12], since the relatively high AMP contamination might prevent synergistic action with cellular ADPR that might have otherwise synergized with cADPR. As the cADPR antagonist 8-Bromo-cADPR is also quite effective in suppressing TRPM2 activation by cADPR (Fig. 3F), one might infer that interference with either ADPR or cADPR prevents synergism of the two compounds and thus preventing any facilitatory effect on TRPM2 activation mediated through these molecules. Interestingly, although TRPM2 in human neutrophils is about 10-fold more sensitive to ADPR than heterologously expressed TRPM2 in HEK293 cells, which have an EC_{50} of 10 μM [7,16] the relative half-maximal inhibitory concentration of AMP in both systems is about 10-fold larger than the EC_{50} for ADPR (HEK293-TRPM2; Fig. 1F and [7]). This indicates that ADPR and AMP compete for the same binding site at the TRPM2 NUDIX domain and that the sensitivity of that binding site to ADPR may differ in TRPM2 channels expressed in different tissues.

ADPR not only synergizes with cADPR to facilitate TRPM2 currents, but also with H_2O_2 and nicotinic acid adenine dinucleotide phosphate (NAADP), the latter being the most powerful Ca^{2+} release agent known to-date [7,10,26]. H_2O_2 has widely been used as activator of TRPM2 for cells expressing this channel [2,8,9], although it should be kept in mind that H_2O_2 also gives rise to a membrane-delimited Ca^{2+}-permeable cation current that is not linked to TRPM2 but most likely due to lipid peroxidation [29]. Nevertheless, while neither 100 μM H_2O_2 nor 100 nM ADPR alone are sufficient to cause TRPM2 activation in human neutrophils, the combination of the two causes TRPM2 currents that are comparable to perfusion with 1 μM ADPR alone, both in terms of amplitude and kinetics of activation (Fig. 3E). This indicates that generation of reactive oxygen species (ROS) will influence TRPM2 activity synergistically rather than be accountable for the overall enhanced ADPR-sensitivity of TRPM2 in neutrophils as compared to HEK293-TRPM2, U937 monocytes or Jurkat T cells [4,7,10].

NAADP is known to be a potent Ca^{2+}-release agent in sea urchin eggs, acting in the low nanomolar range [13]. NAADP does not involve inositol 1,4,5 trisphosphate (IP_3) receptors, but is thought to be due to a novel NAADP receptor in sea urchins [26]. In some eukaryotic cell types, NAADP seems to act on ryanodine-receptor sensitive stores [26]. Furthermore, data from our laboratory implicate TRPM2 as a novel target for NAADP in HEK293 cells overexpressing TRPM2 and native TRPM2 channels in Jurkat T cells [10], albeit at 70-fold lower potency than ADPR. This is also observed in human neutrophils, where TRPM2 currents are activated by NAADP with an EC_{50} of 95 μM (Fig. 4A and D). In addition, NAADP seems to facilitate TRPM2 currents when combined with subthreshold ADPR (100 nM), but only within the narrow concentration range of 0.3 μM to 30 μM NAADP (Fig. 4B and D). ADPR does not seem to shift the dose-response behavior of NAADP at higher concentrations of NAADP (Fig. 4B and D). This behavior may be due to the bell-shaped dose-response curve for NAADP-induced Ca^{2+}-release observed in other cell systems [30-32], where optimal Ca^{2+}-release is elicited by NAADP concentrations between 10 nM and 1 μM, but concentrations above 100 μM NAADP abolish Ca^{2+} release. Thus, lower NAADP concentrations may cause additional Ca^{2+}-release, which in conjunction with subthreshold ADPR facilitates TRPM2 currents in a narrow concentration window. This facilitatory action mediated by Ca^{2+} would then be lost at higher NAADP concentrations even in the presence of subthreshold ADPR ([30-32] and Fig. 4D).

Several dinucleotide-generating pathways have been reported that, in conjunction with ROS production in neutrophils, are well positioned to influence TRPM2-related physiological functions in these cells. CD38, a well-described ADP-ribosyl cyclase also expressed in neutrophils [33], produces mainly ADPR but also cADPR from its substrate NAD^+. However, since CD38 represents an ectoenzyme, it is still unclear how its products might be able to function as intracellular second messengers [27], although recent evidence suggests that nucleoside transporters are responsible for translocating CD38-produced cADPR into human neutrophils causing Ca^{2+} release and migration [34]. On the other hand, there is strong evidence that reactive oxygen species not only liberate ADPR from mitochondria [35], but also cause activation of the DNA repair pathway involving poly(ADP-ribose) polymerase (PARP) and poly(ADP-ribose) glycohydrolase (PARG) with possibly subsequent increases of local ADPR levels acting on TRPM2 [36]. Furthermore, cholecystokinin (CCK) receptor-stimulation has been reported to increase NAADP and cADPR concentrations ultimately altering cellular calcium signals [37]. While human neutrophils are responsive to CCK stimulation, the physiological effect seems rather immunosuppressive than stimulatory in nature [38]. In contrast, a recent report emphasizes the key role of ROS-induced TRPM2 activation in aggravating chemokine-initiated neutrophil infiltration [39].

In conclusion, TRPM2 currents measured in primary human neutrophils are sensitive to internal ADPR levels at physiologically relevant concentrations [12,40], with intracellular Ca^{2+} acting as a mandatory and dose-dependent co-activator of the channel. While cADPR and NAADP activate TRPM2 in neutrophils in the low micromolar range, these agonists may not represent primary or singular activators of TRPM2, but rather work in synergy with ADPR, thus regulating the efficacy and the sensitivity of TRPM2 channels in conjunction with internal Ca^{2+}. Thus, signaling pathways that cause peroxide, cADPR or NAADP generation must be considered regulators of TRPM2. In addition, these agonists synergize with reactive oxygen species, which play an important role in neutrophil function [41] and leukocyte chemotaxis [33,42].

Supplementary Material

Refer to Web version on PubMed Central for supplementary material.

Acknowledgements

We thank Miyoko Bellinger for technical support. Supported by Ingeborg v.F. McKee Fund of Hawaii Community Foundation to John G. Starkus (IL), NIH grants R01-GM063954 (RP) and RO1-GM070634 (AF), Queen Emma Research Foundation Grant No. PA-2006-040 (AB).

References

1. Fleig A, Penner R. The TRPM ion channel subfamily: molecular, biophysical and functional features. Trends Pharmacol Sci 2004;25:633–9. [PubMed: 15530641]
2. Hara Y, Wakamori M, Ishii M, Maeno E, Nishida M, Yoshida T, Yamada H, Shimizu S, Mori E, Kudoh J, Shimizu N, Kurose H, Okada Y, Imoto K, Mori Y. LTRPC2 Ca2+-permeable channel activated by changes in redox status confers susceptibility to cell death. Mol Cell 2002;9:163–73. [PubMed: 11804595]
3. Harteneck C. Function and pharmacology of TRPM cation channels. Naunyn Schmiedebergs Arch Pharmacol 2005;371:307–14. [PubMed: 15843919]
4. Perraud AL, Fleig A, Dunn CA, Bagley LA, Launay P, Schmitz C, Stokes AJ, Zhu Q, Bessman MJ, Penner R, Kinet JP, Scharenberg AM. ADP-ribose gating of the calcium-permeable LTRPC2 channel revealed by Nudix motif homology. Nature 2001;411:595–9. [PubMed: 11385575]
5. Sano Y, Inamura K, Miyake A, Mochizuki S, Yokoi H, Matsushime H, Furuichi K. Immunocyte Ca2 + influx system mediated by LTRPC2. Science 2001;293:1327–30. [PubMed: 11509734]
6. Scharenberg AM. TRPM2 and TRPM7: channel/enzyme fusions to generate novel intracellular sensors. Pflugers Arch 2005;451:220–7. [PubMed: 16001276]
7. Kolisek M, Beck A, Fleig A, Penner R. Cyclic ADP-ribose and hydrogen peroxide synergize with ADP-ribose in the activation of TRPM2 channels. Mol Cell 2005;18:61–9. [PubMed: 15808509]
8. Herson PS, Ashford ML. Activation of a novel non-selective cation channel by alloxan and H2O2 in the rat insulin-secreting cell line CRI-G1. J Physiol 1997;501(Pt 1):59–66. [PubMed: 9174994]
9. Wehage E, Eisfeld J, Heiner I, Jungling E, Zitt C, Luckhoff A. Activation of the cation channel long transient receptor potential channel 2 (LTRPC2) by hydrogen peroxide. A splice variant reveals a mode of activation independent of ADP-ribose. J Biol Chem 2002;277:23150–6. [PubMed: 11960981]
10. Beck A, Kolisek M, Bagley LA, Fleig A, Penner R. Nicotinic acid adenine dinucleotide phosphate and cyclic ADP-ribose regulate TRPM2 channels in T lymphocytes. Faseb J 2006;20:962–4. [PubMed: 16585058]
11. Togashi K, Hara Y, Tominaga T, Higashi T, Konishi Y, Mori Y, Tominaga M. TRPM2 activation by cyclic ADPR-ribose at body temperature is involved in insulin secretion. The EMBO Journal 2006;25:1804–1815. [PubMed: 16601673]
12. Heiner I, Eisfeld J, Warnstedt M, Radukina N, Jungling E, Luckhoff A. Endogenous ADP-ribose enables calcium-regulated cation currents through TRPM2 channels in neutrophil granulocytes. Biochem J 2006;398:225–32. [PubMed: 16719842]
13. Lee HC, Aarhus R. A derivative of NADP mobilizes calcium stores insensitive to inositol trisphosphate and cyclic ADP-ribose. J Biol Chem 1995;270:2152–7. [PubMed: 7836444]
14. Herson PS, Dulock KA, Ashford ML. Characterization of a nicotinamide-adenine dinucleotide-dependent cation channel in the CRI-G1 rat insulinoma cell line. J Physiol 1997;505(Pt 1):65–76. [PubMed: 9409472]
15. McHugh D, Flemming R, Xu SZ, Perraud AL, Beech DJ. Critical intracellular Ca2+ dependence of transient receptor potential melastatin 2 (TRPM2) cation channel activation. J Biol Chem 2003;278:11002–6. [PubMed: 12529379]
16. Starkus J, Beck A, Fleig A, Penner R. Regulation of TRPM2 by Extra- and Intracellular Calcium. J Gen Physiol 2007;130:427–40. [PubMed: 17893195]
17. Tong Q, Zhang W, Conrad K, Mostoller K, Cheung JY, Peterson BZ, Miller BA. Regulation of the transient receptor potential channel TRPM2 by the Ca2+ sensor calmodulin. J Biol Chem 2006;281:9076–85. [PubMed: 16461353]

18. Inamura K, Sano Y, Mochizuki S, Yokoi H, Miyake A, Nozawa K, Kitada C, Matsushime H, Furuichi K. Response to ADP-ribose by activation of TRPM2 in the CRI-G1 insulinoma cell line. J Membr Biol 2003;191:201–7. [PubMed: 12571754]
19. Eisfeld J, Luckhoff A. TRPM2. Handb Exp Pharmacol 2007:237–52. [PubMed: 17217061]
20. Heiner I, Eisfeld J, Halaszovich CR, Wehage E, Jungling E, Zitt C, Luckhoff A. Expression profile of the transient receptor potential (TRP) family in neutrophil granulocytes: evidence for currents through long TRP channel 2 induced by ADP-ribose and NAD. Biochem J 2003;371:1045–53. [PubMed: 12564954]
21. Kraft R, Grimm C, Grosse K, Hoffmann A, Sauerbruch S, Kettenmann H, Schultz G, Harteneck C. Hydrogen peroxide and ADP-ribose induce TRPM2-mediated calcium influx and cation currents in microglia. Am J Physiol Cell Physiol 2004;286:C129–37. [PubMed: 14512294]
22. Carter RN, Tolhurst G, Walmsley G, Vizuete-Forster M, Miller N, Mahaut-Smith MP. Molecular and electrophysiological characterization of transient receptor potential ion channels in the primary murine megakaryocyte. J Physiol 2006;576:151–62. [PubMed: 16857711]
23. Hill K, Tigue NJ, Kelsell RE, Benham CD, McNulty S, Schaefer M, Randall AD. Characterisation of recombinant rat TRPM2 and a TRPM2-like conductance in cultured rat striatal neurones. Neuropharmacology 2006;50:89–97. [PubMed: 16260005]
24. Lipski J, Park TI, Li D, Lee SC, Trevarton AJ, Chung KK, Freestone PS, Bai JZ. Involvement of TRP-like channels in the acute ischemic response of hippocampal CA1 neurons in brain slices. Brain Res 2006;1077:187–99. [PubMed: 16483552]
25. Jamur MC, Grodzki AC, Moreno AN, de Mello Lde F, Pastor MV, Berenstein EH, Siraganian RP, Oliver C. Identification and isolation of rat bone marrow-derived mast cells using the mast cell-specific monoclonal antibody AA4. J Histochem Cytochem 2001;49:219–28. [PubMed: 11156690]
26. Fliegert R, Gasser A, Guse AH. Regulation of calcium signalling by adenine-based second messengers. Biochem Soc Trans 2007;35:109–14. [PubMed: 17233614]
27. Guse AH. Regulation of calcium signaling by the second messenger cyclic adenosine diphosphoribose (cADPR). Curr Mol Med 2004;4:239–48. [PubMed: 15101682]
28. Churamani D, Boulware MJ, Geach TJ, Martin AC, Moy GW, Su YH, Vacquier VD, Marchant JS, Dale L, Patel S. Molecular characterization of a novel intracellular ADP-ribosyl cyclase. PLoS ONE 2007;2:e797. [PubMed: 17726527]
29. Mendez F, Penner R. Near-visible ultraviolet light induces a novel ubiquitous calcium-permeable cation current in mammalian cell lines. J Physiol 1998;507(Pt 2):365–77. [PubMed: 9518699]
30. Berg I, Potter BV, Mayr GW, Guse AH. Nicotinic acid adenine dinucleotide phosphate (NAADP(+)) is an essential regulator of T-lymphocyte Ca(2+)-signaling. J Cell Biol 2000;150:581–8. [PubMed: 10931869]
31. Harmer AR, Gallacher DV, Smith PM. Role of Ins(1,4,5)P3, cADP-ribose and nicotinic acid-adenine dinucleotide phosphate in Ca2+ signalling in mouse submandibular acinar cells. Biochem J 2001;353:555–60. [PubMed: 11171052]
32. Johnson JD, Misler S. Nicotinic acid-adenine dinucleotide phosphate-sensitive calcium stores initiate insulin signaling in human beta cells. Proc Natl Acad Sci U S A 2002;99:14566–71. [PubMed: 12381785]
33. Partida-Sanchez S, Rivero-Nava L, Shi G, Lund FE. CD38: an ecto-enzyme at the crossroads of innate and adaptive immune responses. Adv Exp Med Biol 2007;590:171–183. [PubMed: 17191385]
34. Morita K, Saida M, Morioka N, Kitayama T, Akagawa Y, Dohi T. Cyclic ADP-ribose mediates fromyl methionyl leycil phenylalanine (fMLP)-induced intracellular calcium rise and migration of human neutrophils. J Pharmacol Sci 2008;106:492–504. [PubMed: 18344610]
35. Perraud AL, Takanishi CL, Shen B, Kang S, K SM, Schmitz C, Knowles HM, Ferraris D, Li W, Zhang J, Stoddard BL, Scharenberg AM. Accumulation of free ADP-ribose from mitochondria mediates oxidative stress-induced gating of TRPM2 cation channels. J Biol Chem 2005;18:6138–6148. [PubMed: 15561722]
36. Fonfria E, Marshall IC, Benham CD, Boyfield I, Brown JD, Hill K, Hughes JP, Skaper SD, NcNulty S. TRPM2 channel opening in response to oxidative stress is dependent on activation of poly(ADP-ribose) polymerase. Br J Pharmacol 2004;143:186–192. [PubMed: 15302683]

37. Yamasaki M, Thomas JM, Churchill GC, Garnham C, Lewis AM, Cancela JM, Patel S, Galione A. Role of NAADP and cADPR in the inductin and maintenance of agonist-evoked calcium spiking in mouse pancreatic acinar cells. Curr Biol 2005;15:874–878. [PubMed: 15886108]

38. Carrasco M, Del Rio M, Hernanz A, De La Fuente M. Inhibition of human neutrophil functions by sulfated and nonsulfated cholecystokinin octapeptides. Peptides 1997;18:415–422. [PubMed: 9145430]

39. Yamamoto S, Shimizu S, Kiyonaka S, Takahashi N, Wajima T, Hara Y, Negoro T, Hiroi T, Kiuchi Y, Okada T, Kaneko S, Lange I, Fleig A, Penner R, Nishi M, Takeshima H, Mori Y. TRPM2-mediated calcium influx induces chemokine production in monocytes that aggravates inflammatory neutrophil infiltration. Nat Med. 2008in press

40. Gasser A, Guse AH. Determination of intracellular concentrations of the TRPM2 agonist ADP-ribose by reversed-phase HPLC. J Chromatogr B Analyt Technol Biomed Life Sci 2005;821:181–7.

41. Fialkow L, Wang Y, Downey GP. Reactive oxygen and nitrogen species as signaling molecules regulating neutrophil function. Free Rad Biol Med 2007;42

42. Partida-Sanchez S, Gasser A, Fliegert R, Siebrands CC, Dammermann W, Shi G, Mousseau BJ, Sumoza-Toledo A, Bhagat H, Walseth TF, Guse AH, Lund FE. Chemotaxis of mouse bone marrow neutrophils and dendritic cell is controlled by ADP-ribose, the major product generated by the CD38 enzyme reaction. J Immunol 2007;179:7827–7839. [PubMed: 18025229]

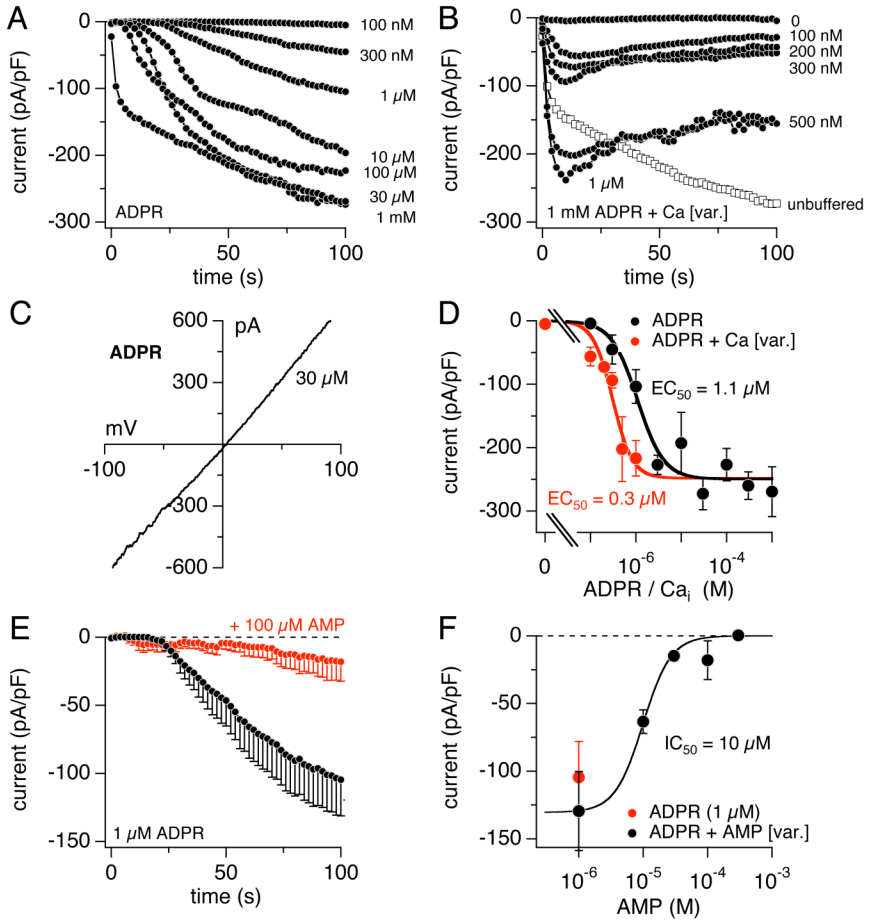

Figure 1. Ca^{2+} facilitates activation of TRPM2 currents in the presence of ADPR

(A) Average normalized TRPM2 currents activated by ADPR in human neutrophils. Currents were measured with a voltage ramp from −100 mV to +100 mV over 50 ms at 0.5 Hz intervals from a holding potential of 0 mV. Inward current amplitudes were extracted at −80 mV, averaged and plotted versus time. Cells were perfused with the standard intracellular K^+-based solution in the absence of exogenous Ca^{2+} buffers and supplemented with increasing ADPR concentrations as indicated (n = 4-10). Standard extracellular solution contained 1 mM Ca^{2+}. **(B)** Average normalized TRPM2 currents activated by 1 mM ADPR and variable intracellular Ca^{2+} concentrations as indicated (n = 5-9). Currents were analyzed as in (A). **(C)** Current-voltage (I/V) curve taken from a representative cell perfused with 30 μM ADPR. **(D)** Dose-response curves of ADPR-induced TRPM2 currents in unbuffered (black circles, n = 4-10) and in clamped Ca^{2+} internal solutions at 1 mM fixed ADPR (red circles, n = 5-9). Data were plotted against ADPR or Ca^{2+} concentrations and fitted with dose-response curves. The EC_{50} values are indicated in the panel. Hill coefficients were 1.5 for unbuffered and 2 for clamped Ca^{2+}. Data were acquired as described in (A). To establish the dose-response curves, the peak inward currents at −80 mV were extracted, averaged and plotted versus the respective ADPR or Ca^{2+} concentration. **(E)** Average normalized TRPM2 inward currents at −80 mV evoked by 1 μM ADPR in the absence (black circles, n = 9) or presence of 100 μM AMP (red circles, n = 6). Error bars represent S.E.M. **(F)** Dose-response curve of TRPM2 currents for AMP in the presence of 1 μM ADPR (black circles, n = 5 - 6). Normalized current amplitudes were measured at 100 s into the experiment, averaged and plotted versus the respective AMP concentration. The data point for 1 μM ADPR in the absence of AMP is plotted in the graph

for reference (red circle, n = 9). A fit to the data gave an IC_{50} of 10 μM AMP with a Hill coefficient of 2.

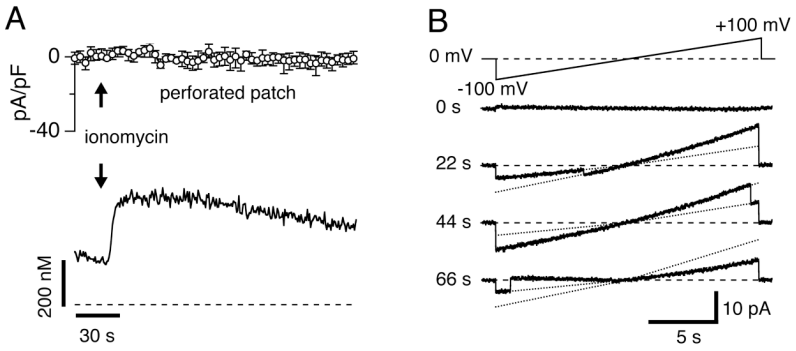

Figure 2. Perforated patch and single-channel experiments

(A) Combined amphotericin-induced perforated-patch and Fura-2 experiments (see methods). The upper trace depicts average perforated-patch whole-cell currents using standard internal solution in the absence of ADPR (n = 3). The lower trace shows the average cellular Ca^{2+} signal measured in parallel in the same cells (n =3). Cells were superfused with standard extracellular solution devoid of Ca^{2+} and supplemented with 2 μM ionomycin for 5 sec as indicated by the two arrows, respectively. Standard voltage ramps were applied from a holding potential of 0 mV. Error bars represent S.E.M. **(B)** Single-channel activity of a representative cell during consecutive voltage ramps applied in the whole-cell configuration. The cell was perfused with 200 nM ADPR and two channels were active (dotted lines indicate channel open levels). A fit to the data gave a single channel conductance of 43 pS ± 0.4 pS (n = 3) at negative potentials and 63 ± 2 pS (n = 3) at positive potentials.

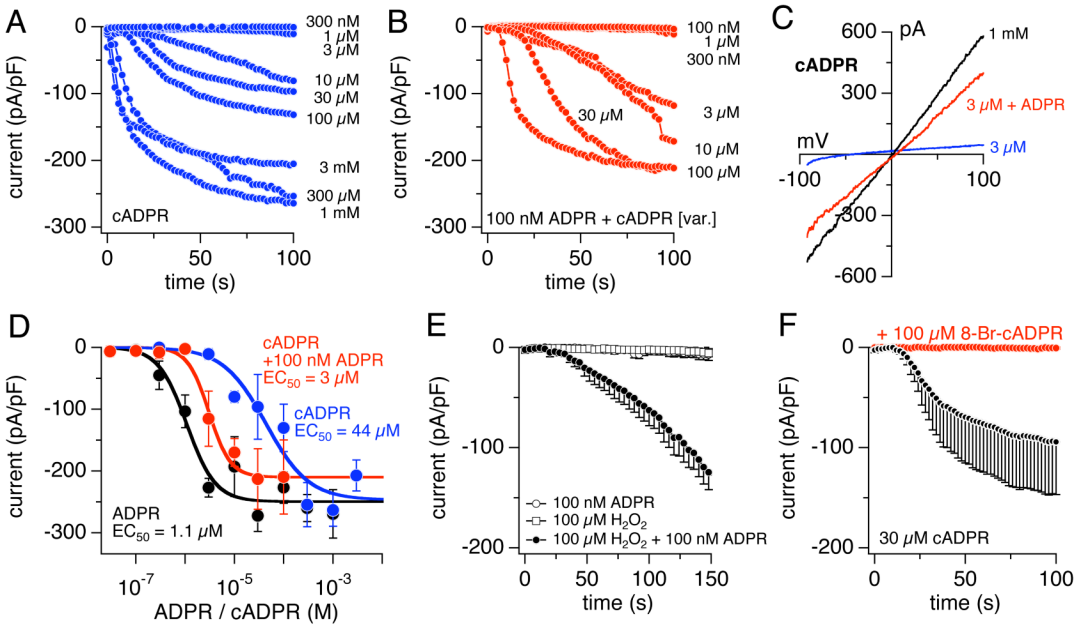

Figure 3. ADPR and cADPR synergize and 8-Bromo-cADPR inhibits TRPM2 currents

(A) Average normalized TRPM2 currents activated by cADPR in human neutrophils (n = 4-9). Intracellular conditions and data acquisition/analysis were as in Fig. 1A. **(B)** Average normalized TRPM2 currents activated by various cADPR concentrations in the presence of 100 nM ADPR (n = 5-7). Intracellular conditions and data acquisition/analysis as in (A). **(C)** I/V curves taken from representative cells perfused with 1 mM cADPR (black trace), 3 μM cADPR (blue trace) or 3 μM cADPR + 100 nM ADPR (red trace). **(D)** Dose-response curves of TRPM2 currents evoked by ADPR (black circles, same data set as in Fig. 1), cADPR (blue circles, n = 4-9) or subthreshold ADPR (100 nM) + increasing cADPR concentrations (red circles, n = 5-7) in unbuffered K^+-based internal solution. Current amplitudes were plotted against concentrations and fitted with dose-response curves. The EC_{50} values are indicated in the panel. Hill coefficients were 1 for cADPR and 2 for cADPR with 100 nM ADPR. To establish the dose-response curves, the peak inward currents at −80 mV were extracted, averaged and plotted versus the respective ADPR or cADPR concentration. **(E)** Average normalized TRPM2 inward currents at −80 mV evoked by 100 nM ADPR and in the absence (open circles, n = 6) or presence of 100 μM H_2O_2 in the patch pipette (closed circles, n = 6). 100 μM H_2O_2 in the pipette without any ADPR did not evoke any currents (open squares, n = 6). Note that the ADPR-only data are overlapping with the H_2O_2 time course and are hidden from view. Error bars represent S.E.M. **(F)** Average normalized TRPM2 inward currents at −80 mV evoked by 30 μM cADPR and in the absence (black circles, n = 7) or presence of 100 μM 8-Br-cADPR (red circles, n = 6). Error bars represent S.E.M.

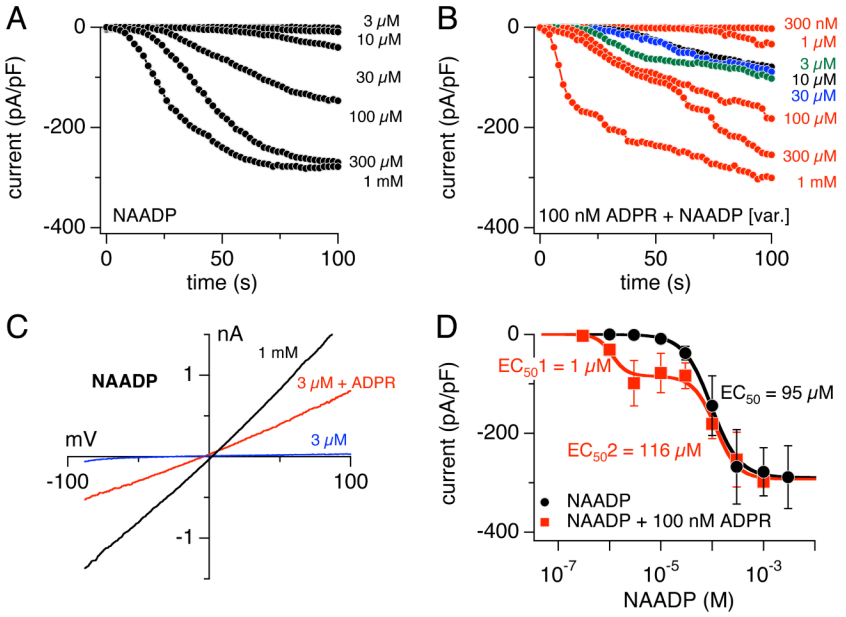

Figure 4. ADPR and NAADP synergize to activate TRPM2 currents

(A) Average normalized TRPM2 currents activated by NAADP in human neutrophils (n = 3-5). Intracellular conditions and data acquisition/analysis were as in Fig. 1A. **(B)** Average normalized TRPM2 currents activated by various NAADP concentrations in the presence of 100 nM ADPR (n = 5-9). Intracellular conditions and data acquisition/analysis as in (A). **(C)** I/V curves taken from representative cells perfused with 1 mM NAADP (black trace), 3 μM NAADP (blue trace) or 3 μM NAADP + 100 nM ADPR (red trace). **(D)** Dose-response curves of TRPM2 currents evoked by NAADP (black circles, n = 3-5) or subthreshold ADPR (100 nM) + increasing NAADP concentrations (red squares, n = 5-9) in unbuffered K^+-based internal solution. Current amplitudes were plotted against concentrations and fitted with dose-response curves. The EC_{50} values are indicated in the panel. Hill coefficient was 1.6 for NAADP. A two-component dose-response curve was fitted to the NAADP data supplemented with 100 nM fixed ADPR. Here, the Hill coefficients were 3 for $EC_{50}1$ and 2 for $EC_{50}2$.

Table 1

EC_{50} values of TRPM2 (in μM) and single-channel conductance (in pS) in different cell types

	HEK293-TRPM2	Neutrophil	Jurkat T	U937	RIN5mf
		In [μM]			
ADPR (BAPTA)	200[f] 90[a] (Cs^+)	No activation[g] (1 mM)	n.d.	130[a] (at 0.1 μM $[Ca^{2+}]_i$, Cs^+)	240 (Cs^+) (Fleig, unpublished)
ADPR unbuffered	10[c,f]	1[e,g] (K^+, Cs^+)	15[d] 7[d] (Cs^+)	40[a] (Cs^+)	20 (Cs^+) (Fleig, unpublished)
cADPR unbuffered	700[c] 120[d] (Cs^+)	44[g]	60[d] (K^+, Cs^+)	n.d.	n.d.
NAADP unbuffered	730[d]	95[g]	Activates[d] (1 mM)	n.d.	n.d.
ADPR [var.] + 10 cADPR unbuffered	0.09[c]	n.d.	Facilitates	n.d.	n.d.
0.1 ADPR + cADPR [var.] unbuffered	n.d.	3[g]	n.d.	n.d.	n.d.
0.1 ADPR + NAADP [var.] unbuffered	n.d.	1[g]	n.d.	n.d.	n.d.
$[Ca^{2+}]_i$	0.05[f] 0.34[b] (Cs^+)	0.3[g]	n.d.	n.d.	n.d.
Single Channel (in pS)	60[a] (Na^+)	56[i] (Cs^+) 43/63[g] (Cs^+)	67[d] (Cs^+)	n.d.	(CRI-G1 cells) 68[h] (Na^+)

Values were assessed in K^+-based intracellular conditions unless indicated otherwise (n.d. = not determined; unbuffered = absence of calcium chelators; [var.] = variable concentrations). Literature:

[a] Perraud et al., 2001;

[b] McHugh et al, 2003;

[c] Kolisek et al, 2005;

[d] Beck et al., 2006;

[e] Heiner et al, 2006;

[f] Starkus et al, 2007;

[g] Lange et al, current manuscript;

[h] Herson & Ashford, 1997;

[i] Heiner et al, 2003.